Carbohydrate Polymers 145 (2016) 1–12

Contents lists available at ScienceDirect

Carbohydrate Polymers

journal homepage: www.elsevier.com/locate/carbpol

# Laccase immobilization on bacterial nanocellulose membranes: Antimicrobial, kinetic and stability properties

Liliana M.P. Sampaio[a,1], Jorge Padrão[b,1], Jorge Faria[a], João P. Silva[b], Carla J. Silva[c], Fernando Dourado[b], Andrea Zille[a,*]

[a] 2C2T—Centre for Textile Science and Technology, Textile Engineering Department, University of Minho, Campus Azurem, 4800-058 Guimarães, Portugal
[b] Centre for Biological Engineering, University of Minho, Campus Gualtar, 4710-057 Braga, Portugal
[c] CeNTI—Centro de Nanotecnologia e Materiais Teícnicos, Funcionais e Inteligentes, Rua Fernando Mesquita 2785, 4760-034 V. N. Famalicão, Portugal

ARTICLE INFO

*Article history:*
Received 30 November 2015
Received in revised form 25 February 2016
Accepted 5 March 2016
Available online 8 March 2016

*Keywords:*
Bacterial cellulose
Laccase
Antimicrobial
Wound dressing
Immobilization
Cytotoxicity

ABSTRACT

This work studied the physical immobilization of a commercial laccase on bacterial nanocellulose (BNC) aiming to identify the laccase antibacterial properties suitable for wound dressings. Physico-chemical analysis demonstrates that the BNC structure is manly formed by pure crystalline Iα cellulose. The pH optimum and activation energy of free laccase depends on the substrate employed corresponding to pH 6, 7, 3 and 57, 22, 48 kJ mol$^{-1}$ for 2,6-dimethylphenol (DMP), catechol and 2,2′-azino-bis-(3-ethylbenzothiazoline-6-sulfonic acid) (ABTS), respectively. The Michaelis–Menten constant (Km) value for the immobilized laccase (0.77 mM) was found to be almost double of that of the free enzyme (0.42 mM). However, the specific activities of immobilized and free laccase are similar suggesting that the cage-like structure of BNC allows entrapped laccase to maintain some flexibility and favour substrate accessibility. The results clearly show the antimicrobial effect of laccase in Gram-positive (92%) and Gram-negative (26%) bacteria and cytotoxicity acceptable for wound dressing applications.


## 1. Introduction

Bacterial nanocellulose (BNC), also known as microbial cellulose or nanocellulose, is a biopolymer synthesized by bacteria belonging to the genera *Acetobacter*, *Gluconacetobacter*, *Rhizobium*, *Agrobacterium* and *Sarcina* (Petersen and Gatenholm, 2011). BNC displays unique structural and mechanical properties as compared with plant cellulose including higher purity, higher crystallinity, higher capacity for water retention, and a three-dimensional nanoscale arrangement of the cellulose fibrils (Römling & Galperin, 2015; Wu & Lia, 2008). BNC aggregates to shape subfibrils, which have a width of around 1.5 nm and are among the thinnest naturally occurring fibres. The size of these fibrils and their spatial arrangement depends on the type of cellulose-synthesizing organism (Mohite & Patil, 2014). Moreover, BNC is nontoxic, noncarcinogenic, biocompatible and exhibits significant bioavailability and biodegradability (in nature) allowing its utilization in the biomedical field for wound dressings, burn treatments, tissue regeneration and as temporary skin substitutes. As a wound dressing, BNC is an excellent material since it provides a moist environment, which is beneficial for the potential transfer of antibiotics or other medicines into the wound environment, while serving as an efficient physical barrier against any external infection. However, BNC per se, lacks antibacterial properties (Shah, Ul-Islam, Khattak, & Park, 2013). A wide range of different strategies has been proposed to inhibit microbial growth and to prevent adverse effects (Banerjee, Pangule, & Kane, 2011; Epstein, Wong, Belisle, Boggs, & Aizenberg, 2012; Lo, Lange, & Chew, 2014). The typical approaches rely either on inhibiting adhesion or on releasing biocidal compounds such as antibiotics, quaternary ammonium salts and silver ions into the surrounding environment, but the emergence of antibiotic- and silver-resistant strains, along with new restrictions on the use of toxic synthetic biocides, forced the development of new strategies (Hasan, Crawford, & Lvanova, 2013). Enzybiotics have been proposed an environmentally safe and interesting alternative as antimicrobial agents. The term enzybiotic was used for the first time in 2001 to designate bacteriophage cell wall-degrading enzymes, including lysins, bacteriocins and lysozymes (Villa &

* Corresponding author. Fax: +351 226099157.
*E-mail addresses:* lilianamargarida.1@gmail.com (L.M.P. Sampaio), padraoj@gmail.com (J. Padrão), pg26020@alunos.uminho.pt (J. Faria), jpsilva@deb.uminho.pt (J.P. Silva), CSilva@centi.pt (C.J. Silva), fdourado@deb.uminho.pt (F. Dourado), azille@2c2t.uminho.pt, andrea.zille@gmail.com (A. Zille).
[1] L.M.P. Sampaio and J. Padrão contributed equally to this work.

http://dx.doi.org/10.1016/j.carbpol.2016.03.009
0144-8617/

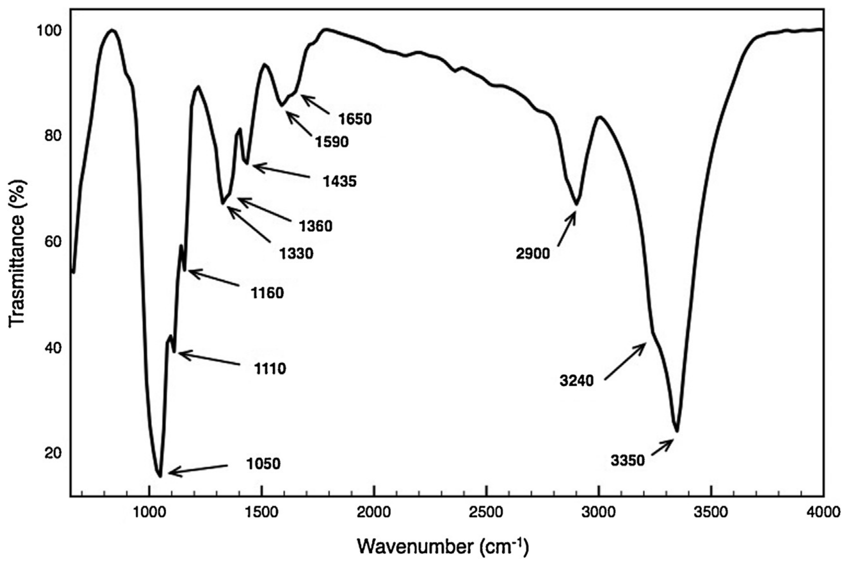


**Fig. 1.** ATR-FTIR spectrum of alkali treated BNC membrane.

Crespo, 2010). However, today it is widely accepted to define all the enzymes displaying antibacterial and even antifungal activity (Ahluwalia & Sekhon, 2012). Enzymes can remove biofilms by cell lysis targeting the cell wall (lysozymes), by degradation of the compounds anchoring cells to the surface such as DNA, proteins and polysaccharides (DNase I, amylases, proteinases), by catalysis of toxic compounds (glucose oxidase, haloperoxidase) or by impairment of intercellular communication (acylase, lactonase) (Glinel, Thebault, Humblot, Pradier, & Jouenne, 2012; Taraszkiewicz, Fila, Grinholc, & Nakonieczna, 2013; Thallinger, Prasetyo, Nyanhongo, & Guebitz, 2013). Oxidoreductases such as glucose oxidase, myeloperoxidase and lactoperoxidase generate hydrogen peroxide ($H_2O_2$) that kills bacterial cells through peroxidation and disruption of cell membranes, oxidation of oxygen scavengers and thiol groups and disruption of protein synthesis. Moreover, they can use $H_2O_2$ as a substrate to oxidize halide/pseudohalide to produce more potent antimicrobials (Thallinger et al., 2013). Among the different existing oxidoreductases, attention has been recently focused on the application of laccases since they have low substrate specificity and do not require the addition of cofactors. Laccases are multicopper oxidases, which not only catalyse the removal of a hydrogen atom from the hydroxyl group of methoxy-substituted monophenols, ortho- and para-diphenols, but also can oxidize other substrates such as aromatic amines, syringaldazine and non-phenolic compounds to form free radicals (Strong & Claus, 2011). Laccases are known to catalyse reactions that lead to the generation of antimicrobial species in the presence of methyl syringate or acetosyringone mediators, phenols, iodine, bromine, hypohalous acid and peracetic acid (Grover, Dinu, Kane, & Dordick, 2013; Kulys, Bratkovskaja, & Vidziunaite, 2005). Interestingly, direct antimicrobial activity of crude laccase against both Gram positive and Gram negative bacteria was also observed and primarily attributed to the electrochemical mode of action to penetrate cell wall of the microorganisms, thereby causing leakage

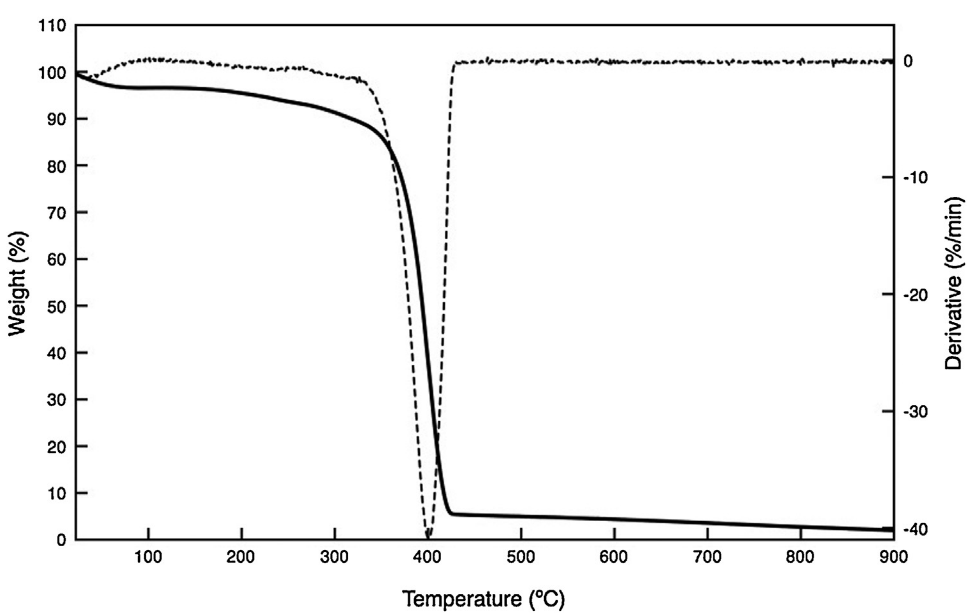


**Fig. 2.** Thermogravimetric analysis (TG) and derivative TG (DTG) of pure alkali-treated BNC from 40 °C to 900 °C. performed at a heating rate of 10 °C $min^{-1}$ under nitrogen atmosphere with a flow rate of 20 mL $min^{-1}$.

of essential metabolites and physically disrupting other microbial key cell functions (Christie & Shanmugam, 2012; Ibrahim, Gouda, El-shafei, & Abdel-Fatah, 2007; Othman et al., 2014).

BNC, due to its mechanical strength, tridimensional nanostructure, high purity, and increased water absorption, can provide an excellent porous ultrafine network structure for laccase immobilization. BNC 3D porous structure allows for high accessibility onto the active site, through low diffusion resistance and easy recoverability as well as potential applicability for continuous operations (Sulaiman, Mokhtar, Naim, Baharuddin, & Sulaiman, 2014). Moreover, the available hydroxyl groups on the surface of nanocellulose provide the possibility of enzyme immobilization by chemical bonds and electrostatic adsorption (Arola, Tammelin, Setälä, Tullila, & Linder, 2012). An effective enzyme immobilization on BNC can be achieved using physical adsorption, entrapment, covalent binding or cross linking (Lin & Dufresne, 2014; Yao, Wu, Zhu, Sun, & Miller, 2013). Despite that, the use of BNC as a support for laccase immobilization is still poorly studied (Frazão et al., 2014; Sathishkumar et al., 2014).

This study develops and optimizes the physical immobilization of a laccase from *Myceliophthora thermophila* onto BNC from *Gluconacetobacter xylinum*. The chemical, mechanical and thermal characteristics of the produced BNC membranes were investigated by thermogravimetry (TGA), differential scanning calorimetry (DSC), and attenuated total reflection Fourier transform infrared spectroscopy (ATR-FTIR) analysis. Free and BNC immobilized laccase were characterized investigating the experimental conditions namely pH, temperature, operational and storage stability and kinetic properties. Finally the in vitro cytotoxicity of laccase immobilized on BNC was examined by measuring the viability of fibroblasts and the antimicrobial effect was evaluated against the medically relevant strains *Staphylococcus aureus* and *Escherichia coli*.

## 2. Material and methods

### 2.1. Materials

Laccase (18 g protein $L^{-1}$) from *M. thermophila* (NS51003, Novozymes, Bagsvaerd, Denmark) was kindly supplied by Professor's Diego Moldes research group from the University of Vigo, Spain. *Gluconacetobacter xylinus* (ATCC 53582) was purchased from the American Type Culture Collection. All the other reagents were analytical grade purchased from Sigma-Aldrich, St. Louis, MO, USA and used without further purification unless stated otherwise.

### 2.2. Silver nanoparticles

Silver nanoparticles (AgNPs) colloidal dispersion with a concentration of 0.02 g $L^{-1}$ was synthetized in laboratory by a modified stepwise method of the conventional reduction technique as previously described (Vu, Zille, Oliveira, Carneiro, & Souto, 2013). During the process the dispersion was mixed vigorously. All solutions of reacting materials were prepared in distilled water. A 100 mL of 1 mM silver nitrate ($AgNO_3$) was heated to boiling in a 250 mL flask. To this solution, 10 mL of 1% trisodium citrate ($Na_3C_6H_5O_7$) were added dropwise (3.8 mM final concentration). The pH value of reaction solution was adjusted by further addition of nitric acid or sodium hydroxide (NaOH) at pH of 7.7. Distilled water was added to restore the initial volume. The solution was heated again to boiling temperature until colour's change was evidenced (pale yellow). Then it was removed from the heating element and stirred until cooled to room temperature. The AgNPs was stored at 4 °C for 12 h before use.

### 2.3. Production of bacterial cellulose

*G. xylinum* was cultured in Hestrin–Schramm medium. Its composition comprised per liter: 20 g of glucose, 5 g peptone and 5 g of yeast extract, 3.4 g of sodium phosphate dibasic dihydrate ($Na_2HPO_4 \cdot 2H_2O$), 1.5 g of citric acid. The medium's final pH was adjusted to 5.5 using hydrochloric acid (HCl) 1 M. A pre-inoculum was prepared from a fresh HS agar plate (HS culture medium supplemented with 2 g $L^{-1}$ of agar) incubated for 5 days at 30 °C. A McFarland 0.5 turbidity standard was used as a reference to inoculate 10 mL of liquid HS medium per well in a 6 well-plate for 21 days, under static conditions at 30 °C. The resulting BNC membranes were rinsed with distilled water, autoclaved at 121 °C at 1.1 bar for 20 min, in order to disrupt the bacteria cells. Afterwards the membranes were immersed into 1 M of sodium hydroxide for 24 h, in order to leach the remaining bacteria debris and culture medium residues from the BNC membranes. Afterwards, BNC membranes were rinsed with distilled water until the pH became equal to the water's pH. The membranes where then cut thinly into 2–3 mm thick membranes. Samples were autoclaved and stored in distilled water at room temperature prior to use.

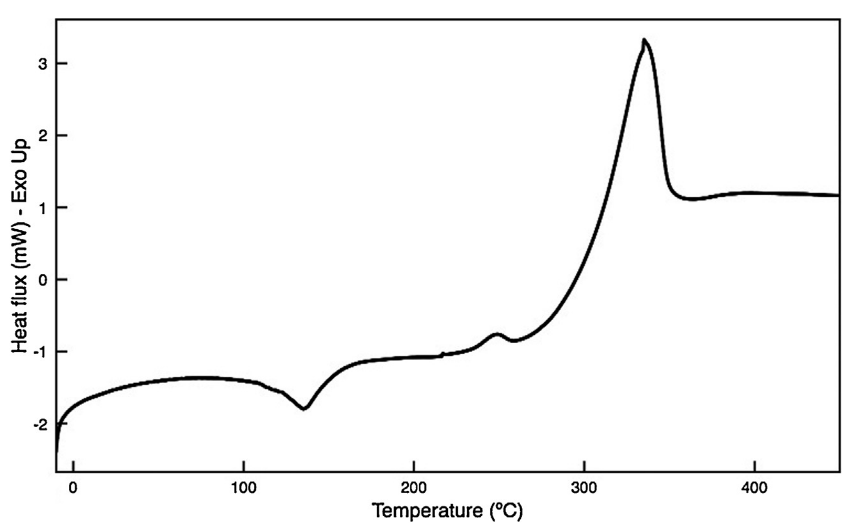


**Fig. 3.** Differential scanning calorimetry (DSC) thermogram of *BNC* from −10 °C to 450 °C performed at a heating rate of 20 °C $min^{-1}$ under nitrogen atmosphere with a flow rate of 20 mL $min^{-1}$.

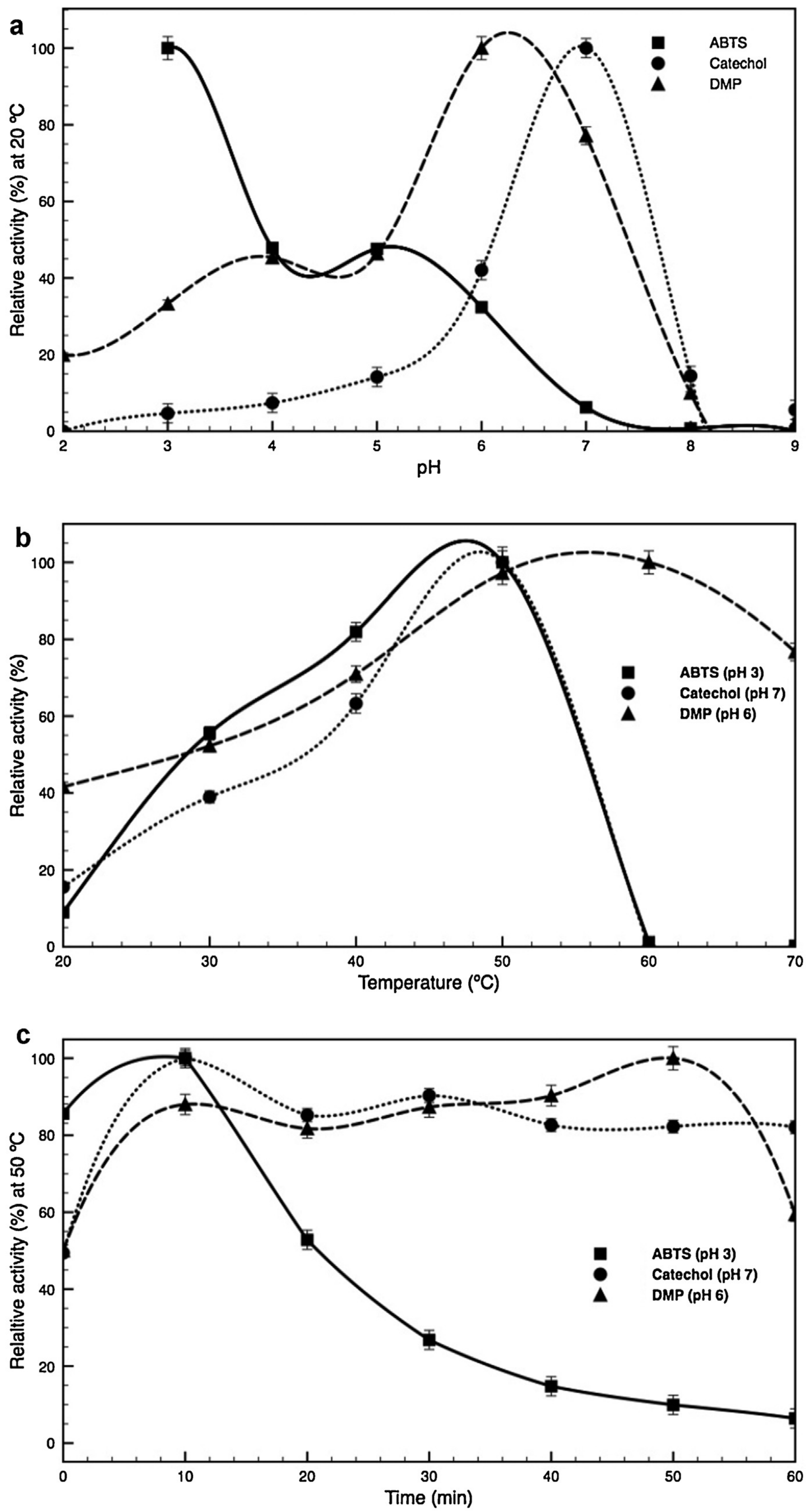


**Fig. 4.** Laccase activity at different pH (a), temperatures (b) and stability at 50 °C under 1 h of incubation (c) for ABTS, DMP and catechol as substrates. Data are presented as average ± standard deviation of three independent measurements.

### 2.4. Thermal gravimetric analysis (TGA)

The thermogravimetric analysis was carried on a Pyris 1 TGA (PerkinElmer, USA), according to the standard ISO 11358:1997(E). The TGA trace was obtained in the range 40–900 °C at a heating rate of 10 °C min$^{-1}$, under nitrogen atmosphere with a flow rate of 20 mL min$^{-1}$. The BNC samples stored in distilled water were lyophilized prior analysis. The lyophilized samples were previously dried at 60 °C for 1 h and placed into a porcelain sample pan. The graph was plotted with weight (percentage) vs. temperatures.

### 2.5. Differential scanning calorimeter analysis (DSC)

The DSC analysis was carried on a Power compensation Diamond DSC (PerkinElmer, USA) with an Intracooler ILP, based on the standards ISO 11357-1:1997, ISO 11357-2:1999 and ISO 11357-3:1999. As above, samples were previously dried at 60 °C for 1 h and placed into an aluminium sample pan. The analysis was carried out in nitrogen atmosphere with a flow rate of 20 mL min$^{-1}$ and heating rate of 10 °C min$^{-1}$. The thermogram of the first heating cycle was obtained in the range of −10 °C to 450 °C, thereafter it was cooled down to −20 °C and heated again to 200 °C. The graph was plotted with heat flow vs. temperatures.

### 2.6. FTIR-attenuated total reflection spectroscopy (ATR-FTIR)

A Nicolet Avatar 360 FTIR spectrophotometer (Madison, USA) with an attenuated total reflectance (ATR) accessory was used to record the FTIR spectra of the membranes, performing 60 scans at a spectral resolution of 16 cm$^{-1}$ over the range 650–4000 cm$^{-1}$. Small squares of lyophilized BNC approximately 16 cm$^2$ was placed onto the crystal using air at 20 °C as background.

### 2.7. Enzyme immobilization

BNC membranes previously stored in distilled water were cut into small squares and lyophilized. Afterwards the membranes were standardized to a weight of 5 mg (~1 cm$^2$) and immersed for 12 h at room temperature in 10 mL laccase preparation diluted 1:100 in 0.1 M phosphate-citrate buffer at pH 3 (1 mL of commercial laccase in 99 mL of buffer). BNC membranes were also immersed in 10 mL laccase preparation diluted 1:10 (1 mL of commercial laccase in 9 mL of buffer) and 1:100 with silver nanoparticles (1 mL of commercial laccase in 99 mL of buffer containing 4 ppm of AgNPs). The amount of protein in the supernatant solution after immobilization was determined by the Bradford assay, using bovine serum albumin as the protein standard. Adsorbed protein was estimated as the difference in weight of the BNC membranes before and after immobilization. The 5 mg BNC membrane weight after immersion in a 1:100 laccase solution was 106 ± 10 mg (average of 10 measures). Thus, the estimated volume of 1:100 laccase solution entrapped in the BNC membrane was 0.1 mL, which correspond to 0.018 mg of protein immobilized in the used membrane. After immobilizations the membranes were immediately used.

### 2.8. Enzyme activity

Laccase activity was determined by measuring the slope of the initial linear portion of the kinetic curve using 2,2′-azino-bis-(3-ethylbenzothiazoline-6-sulfonic acid) (ABTS), catechol and 2,6-dimethylphenol (DMP) as substrates. The reaction was started by adding 1 mL of the enzyme diluted in the appropriate buffer (citrate-phosphate pH 3–6; phosphate pH 7–8; carbonate–bicarbonate pH 9) combined with 1 mL of 0.5 mM substrate reagent (ABTS, DMP or catechol) in a quartz cuvette. The spectrophotometer was zeroed with buffer (1 mL) without enzyme and the substrate (1 mL) (Ander & Messner, 1998; Eichlerova, Snajdr, & Baldrian, 2012). Substrate oxidation was monitored by measuring the absorbance at 450 nm for catechol ($\varepsilon$ = 2211 M$^{-1}$ cm$^{-1}$), at 420 nm for ABTS ($\varepsilon$ = 36000 M$^{-1}$ cm$^{-1}$) and at 468 nm for DMP ($\varepsilon$ = 49600 M$^{-1}$ cm$^{-1}$) and the catalytic activity determined by measuring the slope of the initial linear portion of the kinetic curve. One unit (U) of enzyme activity was defined as the amount of enzyme required to oxidize 1 μmol of used substrates and laccase activities were expressed in μmol min$^{-1}$ mg$^{-1}$ of protein. Protein content in the supernatant solution was determined by the Bradford assay, using bovine serum albumin for the calibration curve (18 mg mL$^{-1}$).

The activity of the immobilized enzymes was calculated using a similar procedure adopted to measure free laccase. The BNC membrane with immobilized laccase (106 mg with an estimated adsorbed volume of 0.1 mL containing 0.018 mg of protein) was

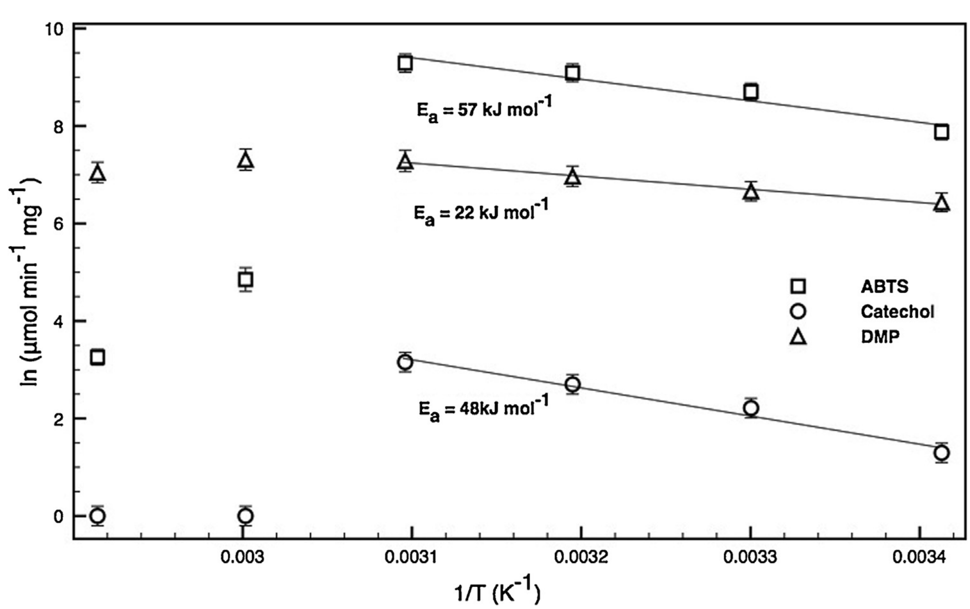


**Fig. 5.** Arrhenius plot with activation energy and breaking points for ABTS (pH 3), DMP (pH 6) and catechol (pH 7) as substrates.

then immersed in a cuvette using 1.9 mL of ABTS solution (1 mM in citrate-phosphate buffer at pH of 3) as substrate for 2 min at 37 °C in a UV–vis spectrophotometer (UV-2 Unicam Instruments, Cambridge, UK). Protein leaching was evaluated by the Bradford assay measuring the amount of protein in the supernatant after the measure of the immobilized enzyme activity. No significant amount of protein was found in the supernatants for all the tested BNC membranes with immobilized laccase. The activity was expressed by the quantity of enzyme capable to oxidize 1 μmol of ABTS per minute and laccase activities were expressed in μmol $min^{-1}$ $mg^{-1}$ of protein (Frazão et al., 2014). Data are presented as average ± SD of three independent measurements.

### 2.9. Enzyme characterization

Free laccase stability at different pH (2–9, using different buffers: citrate-phosphate pH 3–6; phosphate pH 7–8; carbonate–bicarbonate pH 9) and temperatures (20–70 °C) were determined in using ATBS, catechol and DMP as substrates. Laccase activity was expressed as the ratio between the activity at a given time and the initial activity. All activities are presented as average ± SD of three independent measurements. The activation energy ($E_a$) and the break point for the thermal enzyme denaturation process was calculated from the slope of the Arrhenius plot of ln k against 1/T considering the Arrhenius equation:

$$\ln k = \ln A - (E_a/R)(1/T) \quad (1)$$

where $k$ is the reaction rate (μmol $min^{-1}$ $mg^{-1}$). A is the Arrhenius pre-exponential factor (μmol $min^{-1}$ $mg^{-1}$). $R$ is the universal gas constant (8.314 J $mol^{-1}$ $K^{-1}$) and $T$ is the absolute temperature in Kelvin.

### 2.10. Thermal stability of free and immobilized enzyme

The thermal stabilities were investigated by incubating the free and immobilized enzymes in 0.1 M citrate-phosphate buffer (pH 3) for 60 h at 37 °C. Enzymatic activity was measured using ABTS as substrate according to the method described previously in Section 2.7. The thermal parameters were calculated by a non-linear fitting over the experimental data using the non-linear least square-fitting program "Solver" (Excel, Microsoft). During the fitting of the data the inactivation showed to follow a single first-order exponential decay:

$$\text{Relative activity}\,(\%) = (100 - \alpha)e^{-kt} + \alpha \quad (2)$$

where $\alpha$ is the ratio of specific activity, $t$ the time of incubation and $k$ the thermal inactivation rate constant. The half-life times ($t_{1/2}$) was calculated as the $\ln 2/k$.

### 2.11. Kinetic of free and immobilized enzyme

To determine the kinetic parameters of free and immobilized laccase, enzymatic activity was measured for concentrations of ABTS ranging from 0.01 to 4 mM at 37 °C, according to the method described previously in Section 2.7. Non-linear fit of the experimental values to the Michaelis–Menten kinetic model:

$$V = V_{max}\, S/(K_m + S) \quad (3)$$

where $V$ is the reaction velocity (mM $min^{-1}$) and $S$ is the substrate concentration. The kinetic parameters, Michaelis–Menten constant $K_m$ (mM) and the maximum rate of the reaction $V_{max}$ (mM $min^{-1}$), represent the affinity of laccase for the substrate and the maximum reaction velocity, respectively, and were calculated by fitting kinetics data to the model using the non-linear least square-fitting program "Solver" (Excel, Microsoft).

### 2.12. Antimicrobial test

The AATCC Test Method 100-TM100 was adapted to evaluate the contact bactericidal efficiency of BNC and polyamide fabrics. Briefly, BNC disks with 9 mm in diameter, with and without immobilized laccase, were placed in a 48 titration plate, and were inoculated with either $9.7 \times 10^5$ CFU $mL^{-1}$ *S. aureus* or $9.2 \times 10^5$ CFU $mL^{-1}$ of *E. coli*. After 2 h of incubation at 37 °C, 500 μL of PBS the samples were orbital stirred for no less than 1 min, to homogenize the bacterial population. Afterwards, 100 μL of the homogenized solution was retrieved and colony-forming unit per mL (CFU $mL^{-1}$) was determined in MH agar plates as incubated for 24 h at 37 °C, using serial dilutions. The percentage of CFU reduction was determined using the equation:

$$R\% = (A - B)/A\ 100 \quad (4)$$

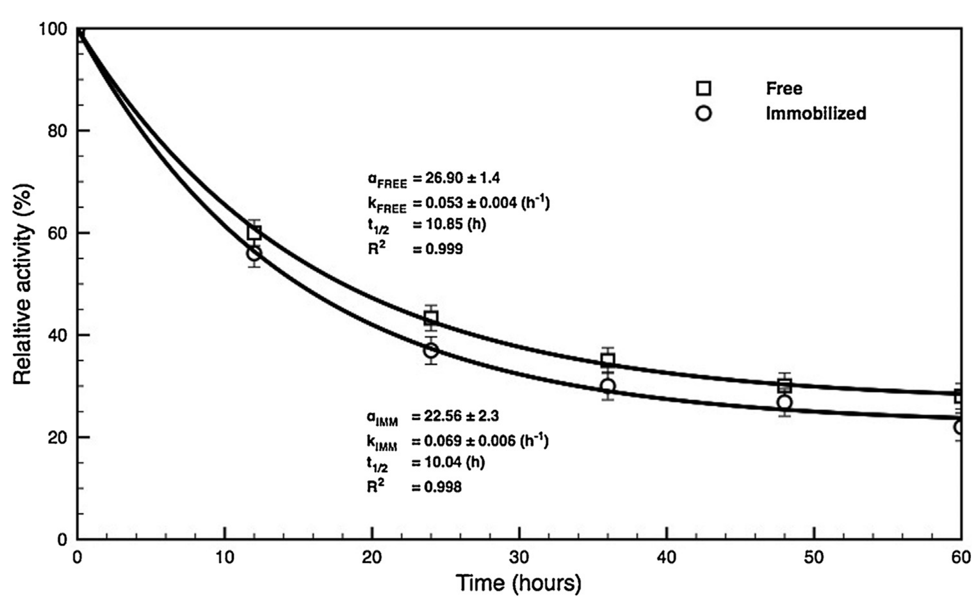


**Fig. 6.** Thermal inactivation of free and immobilized laccase at 37 °C. The solid lines represent the fitting of the single exponential decay model. Data are expressed as mean of three independent assays.

where *R*% represents the percentage of CFU reduction. *A*, the CFU $mL^{-1}$ obtained in for the control samples (BNC) after 2 h of contact, and *B*, the CFU $mL^{-1}$ obtained in BNC samples containing laccase and laccase with silver nanoparticles, after 2 h of contact, at 37 °C. Three BNC disks were used for each studied bacteria. Data are presented as average ± standard error of the mean of three independent measurements.

### 2.13. Cytoxicity test

Cytotoxicity tests were performed using 3T3 mouse embryo fibroblasts (ATCC CCL-164) seeded in a 96-well polystyrene plate (TPP, Switzerland). Cells were incubated in Dulbecco's Modified Eagle's medium (DMEM) (Biochrom.) with 10% (v/v) new-born calf serum (NCS) (Invitrogen) and 1% (v/v) of penicillin/streptomycin at 37 °C in a 5% $CO_2$ humidified atmosphere. The initial cell density used was $7.0 \times 10^4$ cells per well, and the incubation lasted for 72 h at 37 °C in a 5% $CO_2$ humidified atmosphere. Cells seeded on polystyrene were used as a positive control (living cells). BNC sheets were cut into discs (0.5 mm diameter), sterilized by autoclaving and placed in the wells polystyrene plates. Laccase was filtered through 0.2-μm-pore-size membrane filters and then adsorbed into the sterilized BNC. The total number of fibroblasts adhered onto BNC, containing or not laccase were quantified at 0, 24, 48 and 72 h of incubation in the Neubauer chamber, using trypan blue to distinguish viable and non-viable cells. Data are presented as average ± standard error of the mean of seven independent measurements.

## 3. Results and discussion

### 3.1. Bacterial cellulose characterization

#### 3.1.1. ATR-FTIR analysis

The ATR-FTIR spectrum (Fig. 1) of the BNC sample exhibited the characteristic absorption bands of cellulose. The broad and strong band at 3350 $cm^{-1}$ corresponds to the stretching vibration of the hydroxyl (OH) group (Li et al., 2012). The appearance of the shoulder at 3240 $cm^{-1}$ assigned to the triclinic Iα allomorph phase suggests that crystalline cellulose Iα is dominant in this BNC sample (Castro et al., 2011; Nakai et al., 2012). No absorbance bands assigned to the monoclinic Iβ form (3270 and 710 $cm^{-1}$) can be clearly detected in the ATR-FTIR spectrum. The absorption bands at 2900 and 2880 $cm^{-1}$ are assigned to the asymmetrical C—H stretching vibration of aliphatic $CH_2$ and the band at 1435 $cm^{-1}$ to the C—H bending of aliphatic $CH_2$. The peaks at 1360 and 1330 $cm^{-1}$ can be attributed to the $CH_3$ and OH deformational vibrations, respectively (Saska et al., 2012). Furthermore, the very strong bands at 1170, 1110 and 1050 $cm^{-1}$ are assigned to the vibrations of the C—O—C bond of the glycosidic bridges (Algar et al., 2015). The band at 1650 $cm^{-1}$ is due to the bending mode of adsorbed water. The absorption band at 1590 $cm^{-1}$ is attributed to the presence of carboxylic groups suggesting a partial oxidation of the primary hydroxyl groups due to the alkali treatment (Goncalves et al., 2015; Keshk, 2008).

#### 3.1.2. TGA analysis

Native BNC had to be purified to obtain pure cellulose since after fermentation impurities such as proteins, nucleic acids and other media ingredients are embedded within the 3D nanofibrillar matrix. The most used purification method is the alkali treatment as it is capable of efficiently removing and hydrolysing impurities. However, several works available in literature do not perform the required purification step. Raw bacterial cellulose usually shows a TG with three stepwise of weight reduction due to degradation of non-cellulosic materials (Indrarti & Yudianti, 2012). Differently, the alkali-treated BNC displays distinctive thermal properties due to its peculiar morphological and purity characteristics. The TG of alkali-treated BNC in this work shows a two stepwise process of weight reduction indicating an effective impurities removal by the alkali treatment. In the first step the polymer showed an initial small weight loss (7%) due to moisture content between 40 and 100 °C (Fig. 2), even after pre-exposure of the samples to 60 °C for 1 h (as described in Section 2). Above this temperature the weight remains constant until a second phase, attributed to cellulose decomposition that starts at around 370 °C and continues till 417 °C with a major weight loss of about 88%. The highest loss occurs at the maximum decomposition temperature ($T_{max}$) of 395 °C as shown in derivative thermal gravimetric (DTG) curve. It is widely reported in literature that cellulose thermal degradation behaviour is affected by structural parameters such as molecular weight, crystallinity and orientation (Poletto, Júnior, & Zattera, 2014). The removal of BNC impurities by alkaline treatment results in a shift of the maximum decomposition rate to higher temperature indicating a purity and thermal stability improvement (George, Ramana, Sabapathy, Jagannath, & Bawa, 2005). The amount of residue formed by alkali-treated BNC at final decomposition temperature of 900 °C was 2% corresponding to the inorganic components of cellulose (Mohd Amin, Ahmad, Halib, & Ahmad, 2012).

#### 3.1.3. DSC analysis

The DSC first heating cycle was performed from −10 °C to 450 °C, thereafter it was cooled down to −20 °C and heated again to 200 °C. The cooling and second heating cycles do not reveal either crystalline structures or other transitions (data not shown). This may be attributable to the thermal degradation/evaporation during the first heating cycle (Khan et al., 2010). The heat flow curve of the first heating of the alkali treated BNC (Fig. 3) showed an endothermic peak at 135 °C which could be related to bonded water loss or to be the crystalline melting temperature of the polymer (Barud et al., 2011). Moreover, two exothermic peaks were also detected. A small peak at 250 °C that does not correspond to a mass loss and probably it is due to the degradation of the intermolecular hydrogen bonds between BNC nanofibers, and one major peak at around 335 °C attributed to the partial pyrolysis with fragmentation of carbonyl and carboxylic bonds from anhydrous glucose units producing carbon and/or carbon monoxide (Santos et al., 2014). The DSC of BNC does not show any readable $T_g$ features. Despite the high crystallinity, this behaviour is frequently detected in cellulose, due to its rigid-rod polymer backbone having strong inter- and/or intra-molecular hydrogen bonding and to the rigid amorphous phase because of its heterocyclic units (Lee, Kim, & Lee, 2000). As a result, the variations in heat capacity corresponding to the change in specific volume near $T_g$ are difficult to detect properly using DSC because of the broad and flat heat flow curves for which step deviation from the base line is comparatively less (George et al., 2005).

### 3.2. Laccase characterization

The effect of pH, temperature and thermal stability on enzyme activity is reported in Fig. 4. The pH optimum (Fig. 4a) of the *M. thermophila* laccase depends on the substrate employed and shows a bell-shaped pH activity profile with an optimum of 6 (DMP) to 7 (catechol) for the phenolic substrates, while the non-phenolic substrate ABTS with a pH optimum of 3 (no activity was observed at pH 2) shows a monotonic pH activity profile that decrease with the increase in pH (Dube, Shareck, Hurtubise, Daneault, & Beauregard, 2008). The differences in pH optima between ABTS and phenolic substrates reflect the difference in oxidation mechanism with different substrates (Chakroun, Mechichi, Martinez, Dhouib, & Sayadi, 2010). In general, the catalytic activity of laccase shows a bell-

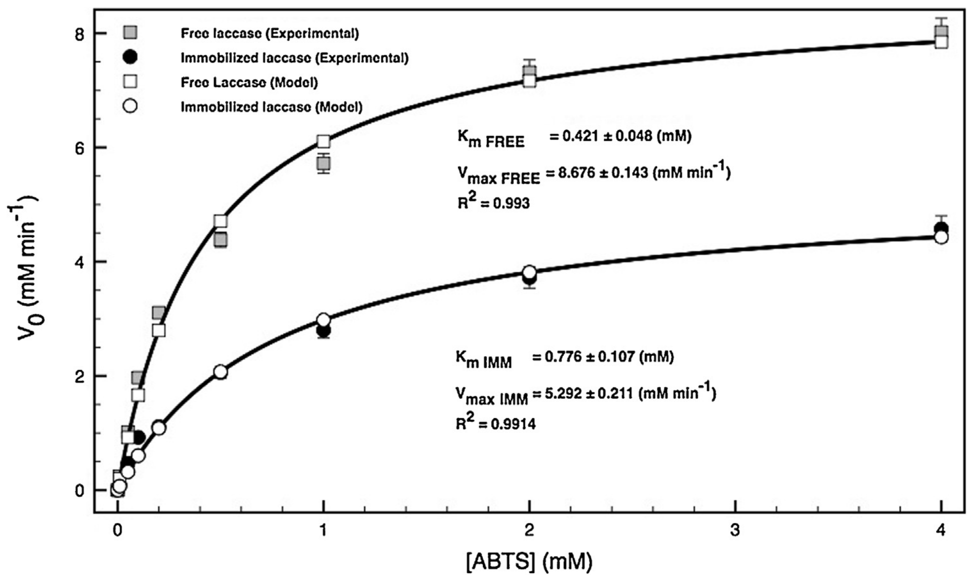


**Fig. 7.** Initial reaction rates for different concentrations of ABTS with and immobilized laccase on BNC at 37 °C. The solid lines represent the fitting of Michaelis–Menten model to experimental data. Data are expressed as mean of three independent assays.

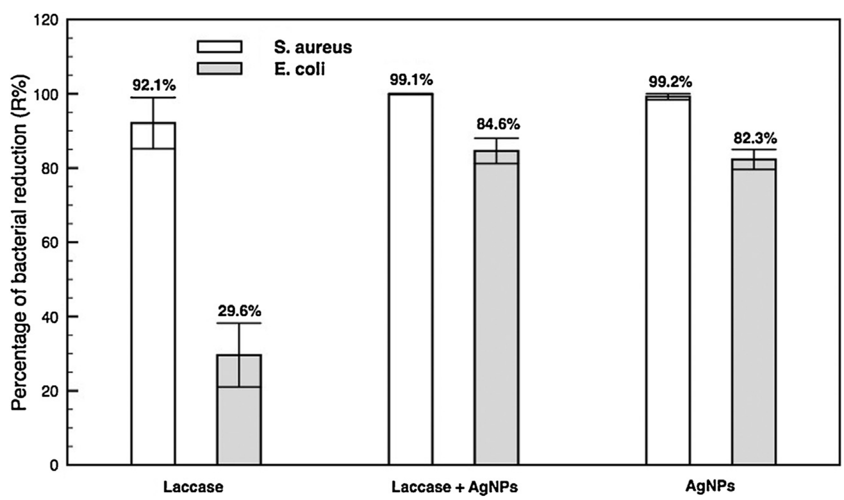


**Fig. 8.** *Escherichia coli* and *Staphylococcus aureus* growth reduction of BNC immobilized laccase. Silver nanoparticles (AgNPs) and laccase + AgNPs respect to the pure BNC membrane as control. Data are presented as average ± standard error of the mean of three independent measurements.

shaped pH profile for the majority of substrates which is mainly due to the $OH^-$ inhibition at higher pH and to the pH-dependent redox potential of the substrate at intermediate pH (Jimenez-Juarez et al., 2005). In the case of ABTS the monotonic pH profile depends exclusively by the $OH^-$ inhibition because the formation of cation radical does not involve proton transfer and the redox potential of ABTS is pH independent (Quan, Kim, & Shin, 2004). However, the ionic composition of the buffer can also has a critical effect on enzyme activity and could explain the plateau observed between pH 4 and 5 for DMP and ABTS (Turner, 2010). Table 1 presents the specific activities of *M. thermophila* laccase with the used substrates. The specific activity was highest with ABTS at 50 °C (601.6 U $mg^{-1}$ at pH 3). The other typical substrates for laccases DMP and catechol were also oxidized showing a discrete activity of 83.2 U $mg^{-1}$ for DMP at pH 6 while catechol presents the lowest activity with 16 U $mg^{-1}$ at its optimum pH of 7. The thermal profile of the enzyme shows an optimum around 50 °C for all the used substrates however, ABTS and catechol activities declined sharply above this value (Fig. 4b). With DMP, activity remained steady up to 70 °C then also underwent a sharp decline. The assays performed to assess the enzyme thermal stability confirmed its thermostability (Fig. 4c) as previously reported, retaining 80% of its initial activity after 1 h of incubation at 50 °C for the phenolic substrates (Chakroun et al., 2010; Ibarra, Romero, Martínez, Martínez, & Camarero, 2006). However, in the case of ABTS as substrates the enzyme exhibits a short half-life retaining only 10% activity after 60 min of incubation. Because of its thermostability for phenolic substrates and superior performance in a broad pH range (especially at alkaline pH), *M. thermophila* laccase is an excellent enzyme for various potential industrial applications,

**Table 1**
Specific activity of *M. thermophila* laccase towards ABTS, DMP and catechol in function of their optimum pH at 25, 37 and 50 °C. Data are presented as average ± standard deviation of three independent measurements.

| | Specific activity (U $mg^{-1}$) | | |
|---|---|---|---|
| | ABTS (pH 3) | Catechol (pH 7) | DMP (pH 6) |
| 25 °C | 293.3 ± 11.2 | 1.3 ± 0.4 | 43.4 ± 3.2 |
| 37 °C | 493.0 ± 9.5 | 2.3 ± 0.5 | 58.9 ± 3.0 |
| 50 °C | 601.6 ± 23.5 | 16.0 ± 1.7 | 83.2 ± 10.8 |

including medical uses (Grover, Borkar, Dinu, Kane, & Dordick, 2012).

To analyse the effect of temperature on the stabilization rate of laccase in function of the substrates the Arrhenius plot is exhibited in Fig. 5. The plot reveals two distinct linear parts (or a nonlinear plot) with different slopes with a break point at 50 °C for all the used substrates. ABTS and catechol showed a sharp break after 50 °C, while DMP display just a slight change in slope. There are a number of factors that can be responsible for nonlinear Arrhenius plots, such as changes in the ionization state of the enzyme due to changes in the pH, reversible inactivation of the enzyme due to purely kinetic phenomena or temperature-induced conformational changes in the enzyme structure (Moosavi-Nejad, Rezaei-Tavirani, Padiglia, Floris, & Moosavi-Movahedi, 2001). Probably, DMP promote lesser conformational changes at high temperature then ABTS and catechol. However, the reason for these sudden variations is still unclear (Poonkuzhali, Sathishkumar, Boopathy, & Palvannan, 2011). The activation energy ($E_a$) was obtained by nonlinear regression of the kinetic constants from the slope of the straight-line plot produced by the Arrhenius equation (Eq. (1)) between 20 and 50 °C. The activation energies of ABTS and catechol were 57 and 48 kJ mol$^{-1}$, respectively. These values are well within the range of other laccase-catalysed reactions (Di Nardo, Cinquegrana, Papa, Fuggi, & Fioretto, 2004). DMP shows a low $E_a$ of 22 kJ mol$^{-1}$ in agreement with other low values observed for diffusion-controlled reactions using *M. thermophila* laccase (López-Cruz, Viniegra-González, & Hernández-Arana, 2006). This seems to indicate a better structural/conformational accommodation in the active site for DMP which renders *M. thermophila* laccase more stable and efficient in binding DMP despite its lower specific activity compared to ABTS (Mukhopadhyay, Dasgupta, & Chakrabarti, 2013).

### 3.3. Laccase immobilization on BNC

As previously established, *M. thermophila* laccase is able to degrade a wide range of phenolic compounds, however it is important to characterize the immobilization effects under good measurable operating conditions by selecting a substrate with quantifiable reactivity (Chea, Paolucci-Jeanjean, Sanchez, & Belleville, 2014). Thus, ABTS was chosen to compare free and immobilized enzyme catalysis due to its higher specific activity compared to phenol-based substrates. Moreover, since it was extensively reported that the pH profile of the immobilized laccase in BNC was closely similar to that of the soluble enzyme, both the free and immobilized laccase was performed at the same optimum pH of free ABTS (pH 3) and at the physiological temperature of 37 °C (Frazão et al., 2014; Wu & Lia, 2008).

Thermal stability is one of the most important features for the application of immobilized biocatalyst. In the present work, the heat deactivation for both free and immobilized enzymes was adequately represented by a classical first-order (single exponential decay) model (Fig. 6). The half-life time ($t_{1/2}$), which corresponds to the time necessary for the residual enzyme activity to decrease to 50% of its initial value at a certain temperature, was practically the same for free and immobilized enzyme (10.8 and 10 h, respectively) while, the thermal deactivation rate constant ($k$) of the immobilized laccase (0.069 h$^{-1}$) is higher than the free enzyme (0.053 h$^{-1}$). Thermal inactivation rate constant ($k$) and observed half-life ($t_{1/2}$) values show that, thermal stability of laccase is not improved after immobilization procedure. This result is not in accordance with most of the literature on laccase immobilization (Frazão, et al., 2014). Usually it is expected an increased in stability due to the enzyme support binding that increase rigidity and contributes to the stabilization of three-dimensional structure of the immobilized enzyme towards denaturation (Cristóvão et al., 2012). Also, the ratio of specific activity ($\alpha$) decrease after laccase immobilization (from 26.9 to 22.5) indicating that the immobilization of laccase is not able to improve the residual thermal stability. After incubation at 37 °C for 60 h, the free enzyme retained an activity of 28% while the immobilized laccase 24%. Although the immobilized laccase displayed a slightly lower thermal stability than the free enzyme, its specific activity is close to that of the free enzymes. The measured specific activity (~400 U mg$^{-1}$ of protein) of immobilized laccase retains about 70% of the native activity at 37 °C. It seems that the structure of BNC hydrogel allows the enzyme to maintain some flexibility and facilitate the diffusion of the substrate, leading to an activity of immobilized enzyme similar to that of the free one. Bacterial cellulose fibrils are about 100 times thinner than that of plant cellulose, making it a highly porous material (Chawla, Bajaj, Survase, & Singhal, 2009). Bacterial cellulose has been suggested to have a cage-like structure, which could efficiently entrap the enzymes without covalent binding, while still allowing substrate to diffuse easily with only a minor loss in activity due to the different diffusion rate and microenvironment variations (Lynd, Weimer, van Zyl, & Pretorius, 2002). This is also proved by the absence of obverse protein leach during the measure of the immobilized enzyme activity. The micropored structures of BNC hydrogel could favour mass transport and accessibility of enzymes to the hydrophilic and hydrophobic domains of cellulose distributed throughout the inner structure but at the expense of the thermostability effect usually attained by other immobilization methods (Nieto et al., 2010).

The enzyme kinetics parameters, maximum reaction rate ($V_{max}$) and apparent Michaelis–Menten constant ($K_m$), of free and immobilized laccase were obtained using the initial reaction rates of ABTS oxidation at different substrate concentrations and fitting the experimental data to the classical Michaelis–Menten model. The non-linear regression analysis showed good fit quality with high values of $R^2$ for both free and immobilized laccase (Fig. 7). The kinetic constant $K_m$ is a measure of the affinity that an enzyme has for a given substrate. The lower the value of $K_m$, the higher is the affinity of the enzyme to the substrate. The $K_m$ value for the immobilized laccase (0.77 mM) was found to be almost double than that of the free laccase (0.42 mM) demonstrating a lower affinity for the substrate. Moreover, the $V_{max}$ of the immobilized laccase (5.29 mM min$^{-1}$) was lower than that of free laccase (8.7 mM min$^{-1}$). The shift of $K_m$ and $V_{max}$ values suggests a lower substrate affinity for the immobilized enzyme as compared to the free enzyme. A lower affinity for the substrate for an immobilized enzyme could be caused by diffusional limitations, decreased enzyme flexibility or lower accessibility of the substrate to the active site (Cristóvão et al., 2012). However, due to the similar previously observed thermal inactivation rate constant ($k$) and half-life ($t_{1/2}$) the diffusional substrate limitations of the laccase penetrated in the BNC structure seem to be the most plausible explanation (Frazão et al., 2014). Similar results were observed in previous studies using BNC as a support for laccase immobilization (Sathishkumar et al., 2014; Tavares et al., 2015).

### 3.4. Antimicrobial properties and cytotoxicity of immobilized laccase

The laccase immobilized onto BNC was tested for its antimicrobial activity against Gram-positive and Gram-negative bacteria and compared with silver nanoparticles (AgNPs) and Laccase/AgNPs immobilized on BNC (Fig. 8). The results clearly show the antimicrobial effect of laccase. Moreover, Gram-positive bacteria were more sensitive to laccase than Gram-negative ones displaying respectively about 92% (*S. aureus*) and 26% (*E. coli*) of bacterial inhibition. Also AgNPs are more efficient against *S. aureus* (99%) than *E. coli* (82%) as previously observed (Zille et al., 2015). The BNC with immobilized laccase and AgNPs has shown the same behaviour

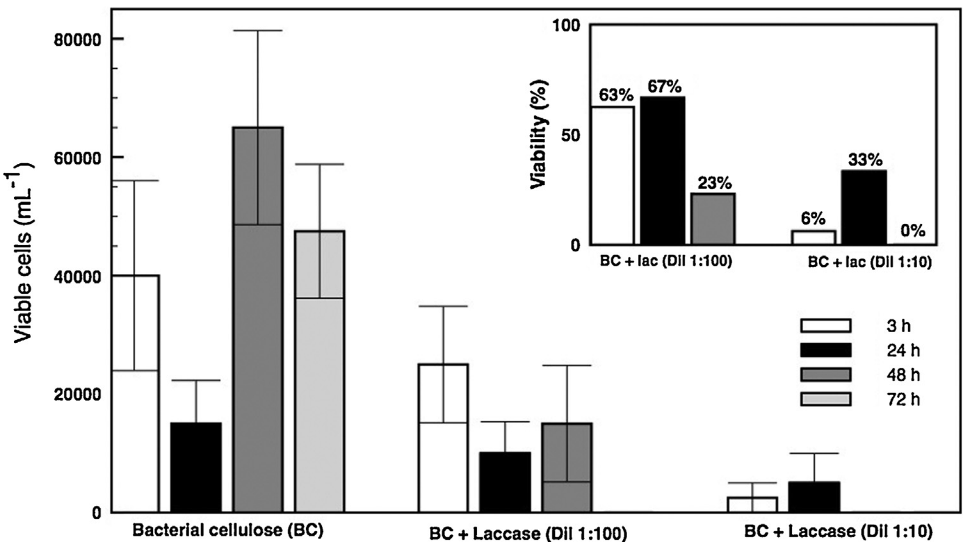


**Fig. 9.** BNC cytotoxicity and viability (inset) with different laccase concentrations. Data are presented as average ± standard error of the mean of seven independent measurements.

of AgNPs probably due to enzyme inactivation. The highest Gram-positive *S. aureus* inhibition could be attributed to the well-known differences in structure and composition of the Gram-positive and Gram-negative bacteria cell wall. The cell wall of Gram-positive bacteria is composed of a thick peptidoglycan layer while, Gram-negative cell wall is more structurally and chemically complex than Gram-positive and it is constituted by a thin peptidoglycan layer and by a lipopolysaccharidic outer membrane, which is unique to Gram-negative bacteria, and can act as a protective barrier against laccase mode of action (Hajipour et al., 2012). It was previously reported that laccase alone is able to efficiently inhibit both Gram-positive and Gram-negative bacteria. However, a very few studies are available in the literature that propose a mechanism of action by laccases. Indeed these enzymes can catalyse the oxidation of a wide variety of amino and phenolic substrates. They reduce oxygen to water but do not produce $H_2O_2$ (Grover et al., 2012; Ibrahim et al., 2007; Othman et al., 2014). The most promising hypothesis explaining laccase's antimicrobial activity, is based on its electrochemical mode of action to penetrate cell wall of microorganisms, thereby causing leakage of essential metabolites and physically disrupting other key cell functions (Othman et al., 2014).

The cytotoxicity of laccase immobilized on BNC was examined by measuring the viability of fibroblasts attached on the membranes using the viable cells on BNC as control (Fig. 9). Laccase exerted some cytotoxic effect on fibroblasts. After 24 h the number of cells on laccase-immobilized BNC membranes (Dil 1:100) was about 70%. The lower viability may be related to the unknown species generated due to the laccase mode of action. Nevertheless, a 30% reduction is considered acceptable for wound dressing applications (Jayakumar, Prabaharan, Sudheesh Kumar, Nair, & Tamura, 2011). On the other hand, the laccase cytotoxicity increased considerably when a dilution 1:10 was used displaying a cell viability of about 30%. After 48 h the observed viabilities were 23% and 0% for laccase dilutions of 1:100 and 1:10, respectively. Cell adhesion is a multiple-step process involving the adsorption of binding proteins, recognition of extracellular matrix, and rearrangement of cytoskeleton (Lin, Lien, Yeh, Yu, & Hsu, 2013). However, further investigation is needed since other unknown factors could affect the cell adhesion on immobilized-laccase BNC membranes.

## 4. Conclusions

In this study a *M. thermophila* laccase was immobilized onto BNC for biomedical purposes as wound dressings. The study on the physico-chemical properties of BNC demonstrate that the BNC structure is manly formed by pure crystalline I$\alpha$ cellulose in which the primary hydroxyl groups are partially oxidised due to the alkali treatment. Laccase activity characterization in function of pH, temperature and thermal stability showed that the optimum pH depends on the employed substrate with higher thermal stability for the phenolic substrates than for ABTS. The activation energies suggest a better conformational accommodation in the active site for DMP. Thermal inactivation rate constant and observed half-life values show that, thermal stability of laccase is not improved after immobilization procedure. The enzyme kinetics parameters of free and immobilized laccase suggest a lower substrate affinity for the immobilized enzyme as compared to the free enzyme due to diffusional substrate limitations of the laccase penetrated in the BNC structure. However, the specific activity of immobilized laccase is close to the free enzymes suggesting that the cage-like structure of BNC allows entrapped laccase to maintain some flexibility and favour mass transport and accessibility of the substrate. The laccase immobilized onto BNC clearly show and antimicrobial effect, being more sensitive for Gram-positive bacteria than Gram-negative ones due to the different electrochemical mode of action of laccase to penetrate the different structure and composition of the Gram-positive and Gram-negative cell walls. Laccase exerted a small cytotoxic effect on fibroblasts but is considered acceptable for wound dressing applications. Since in average a dressing is changed every 1–3 days depending on the amount of exudate, the use of laccase can be considered an efficient, non-toxic, durable and cost-effective antimicrobial agents even if the enzyme quickly lose stability. To maximize stability and shelf life, BNC and laccase can be stored separately until used, due to the simple immobilization procedure that require a unique immersion step.

## Acknowledgements

Andrea Zille (C2011-UMINHO-2C2T-01) acknowledges FCT funding from Programa Compromisso para a Ciência 2008, Portugal, FEDER funding on the Programa Operacional Factores de Competitividade—COMPETE and by national funds through FCT –

Foundation for Science and Technology within the scope of the project POCI-01-0145-FEDER-007136 and UID/CTM/00264. Jorge Padrão and João P. Silva acknowledge Portuguese Foundation for Science and Technology (FCT) grants SFRH/BD/64901/2009 and SFRH/BPD/64958/2009 respectively. The authors Jorge Padrão, João P. Silva and Fernando Dourado would like to thank the FCT Strategic Project PEst-OE/EQB/LA0023/2013, also to the Project "BioHealth – Biotechnology and Bioengineering approaches to improve health quality", Ref. NORTE-07-0124-FEDER-000027, co-funded by the Programa Operacional Regional do Norte (ON.2-O Novo Norte), QREN, FEDER, and finnally to RECI/BBB-EBI/0179/2012 (FCOMP-01-0124-FEDER-027462).

## References

Ahluwalia, A. K., & Sekhon, B. S. (2012). Enzybiotics: a promising approach to fight infectious diseases and an upcoming need for future. *Journal of Pharmaceutical Education and Research*, *3*(2), 42–51.

Algar, I., Fernandes, S. C. M., Mondragon, G., Castro, C., Garcia-Astrain, C., Gabilondo, N., et al. (2015). Pineapple agroindustrial residues for the production of high value bacterial cellulose with different morphologies. *Journal of Applied Polymer Science*, *132*(1), 41237.

Ander, P., & Messner, K. (1998). Oxidation of 1-hydroxybenzotriazole by laccase and lignin peroxidase. *Biotechnology Techniques*, *12*(3), 191–195.

Arola, S., Tammelin, T., Setälä, H., Tullila, A., & Linder, M. B. (2012). Immobilization—stabilization of proteins on nanofibrillated cellulose derivatives and their bioactive film formation. *Biomacromolecules*, *13*(3), 594–603.

Banerjee, I., Pangule, R. C., & Kane, R. S. (2011). Antifouling coatings: recent developments in the design of surfaces that prevent fouling by proteins, bacteria, and marine organisms. *Advanced Materials*, *23*(6), 690–718.

Barud, H. S., Souza, J. L., Santos, D. B., Crespi, M. S., Ribeiro, C. A., Messaddeq, Y., et al. (2011). Bacterial cellulose/poly(3-hydroxybutyrate) composite membranes. *Carbohydrate Polymers*, *83*(3), 1279–1284.

Castro, C., Zuluaga, R., Putaux, J.-L., Caro, G., Mondragon, I., & Gañán, P. (2011). Structural characterization of bacterial cellulose produced by *Gluconacetobacter swingsii* sp. from Colombian agroindustrial wastes. *Carbohydrate Polymers*, *84*(1), 96–102.

Chakroun, H., Mechichi, T., Martinez, M. J., Dhouib, A., & Sayadi, S. (2010). Purification and characterization of a novel laccase from the ascomycete *Trichoderma atroviride*: application on bioremediation of phenolic compounds. *Process Biochemistry*, *45*(4), 507–513.

Chawla, P. R., Bajaj, I. B., Survase, S. A., & Singhal, R. S. (2009). Microbial cellulose: fermentative production and applications. *Food Technology and Biotechnology*, *47*(2), 107–124.

Chea, V., Paolucci-Jeanjean, D., Sanchez, J., & Belleville, M.-P. (2014). Potentialities of a membrane reactor with laccase grafted membranes for the enzymatic degradation of phenolic compounds in water. *Membranes*, *4*(4), 678–691.

Christie, S., & Shanmugam, S. (2012). Analysis of fungal cultures isolated from Anamalai Hills for laccase enzyme production effect on dye decolorization, antimicrobial activity. *International Journal of Plant, Animal and Environmental Sciences*, *2*(3), 143–148.

Cristóvão, R. O., Silvério, S. C., Tavares, A. P. M., Brígida, A. I. S., Loureiro, J. M., Boaventura, R. A. R., et al. (2012). Green coconut fiber: a novel carrier for the immobilization of commercial laccase by covalent attachment for textile dyes decolourization. *World Journal of Microbiology and Biotechnology*, *28*(9), 2827–2838.

Di Nardo, C., Cinquegrana, A., Papa, S., Fuggi, A., & Fioretto, A. (2004). Laccase and peroxidase isoenzymes during leaf litter decomposition of *Quercus ilex* in a Mediterranean ecosystem. *Soil Biology and Biochemistry*, *36*(10), 1539–1544.

Dube, E., Shareck, F., Hurtubise, Y., Daneault, C., & Beauregard, M. (2008). Homologous cloning, expression, and characterisation of a laccase from *Streptomyces coelicolor* and enzymatic decolourisation of an indigo dye. *Applied Microbiology and Biotechnology*, *79*(4), 597–603.

Eichlerova, I., Snajdr, J., & Baldrian, P. (2012). Laccase activity in soils: considerations for the measurement of enzyme activity. *Chemosphere*, *88*(10), 1154–1160.

Epstein, A. K., Wong, T. S., Belisle, R. A., Boggs, E. M., & Aizenberg, J. (2012). Liquid-infused structured surfaces with exceptional anti-biofouling performance. *Proceedings of the National Academy of Sciences*, *109*(33), 13182–13187.

Frazão, C. J. R., Silva, N. H. C., Freire, C. S. R., Silvestre, A. J. D., Xavier, A. M. R. B., & Tavares, A. P. M. (2014). Bacterial cellulose as carrier for immobilization of laccase: optimization and characterization. *Engineering in Life Sciences*, *14*(5), 500–508.

George, J., Ramana, K. V., Sabapathy, S. N., Jagannath, J. H., & Bawa, A. S. (2005). Characterization of chemically treated bacterial (*Acetobacter xylinum*) biopolymer: some thermo-mechanical properties. *International Journal of Biological Macromolecules*, *37*(4), 189–194.

Glinel, K., Thebault, P., Humblot, V., Pradier, C. M., & Jouenne, T. (2012). Antibacterial surfaces developed from bio-inspired approaches. *Acta Biomaterialia*, *8*(5), 1670–1684.

Goncalves, S., Padrao, J., Rodrigues, I. P., Silva, J. P., Sencadas, V., Lanceros-Mendez, S., et al. (2015). Bacterial cellulose as a support for the growth of retinal pigment epithelium. *Biomacromolecules*, *16*(4), 1341–1351.

Grover, N., Borkar, I. V., Dinu, C. Z., Kane, R. S., & Dordick, J. S. (2012). Laccase- and chloroperoxidase-nanotube paint composites with bactericidal and sporicidal activity. *Enzyme and Microbial Technology*, *50*(6–7), 271–279.

Grover, N., Dinu, C. Z., Kane, R. S., & Dordick, J. S. (2013). Enzyme-based formulations for decontamination: current state and perspectives. *Applied Microbiology and Biotechnology*, *97*(8), 3293–3300.

Hajipour, M. J., Fromm, K. M., Akbar Ashkarran, A., Jimenez de Aberasturi, D., Larramendi, I. R. d., Rojo, T., et al. (2012). Antibacterial properties of nanoparticles. *Trends in Biotechnology*, *30*(10), 499–511.

Hasan, J., Crawford, R. J., & Lvanova, E. P. (2013). Antibacterial surfaces: the quest for a new generation of biomaterials. *Trends in Biotechnology*, *31*(5), 31–40.

Ibarra, D., Romero, J., Martínez, M. J., Martínez, A. T., & Camarero, S. (2006). Exploring the enzymatic parameters for optimal delignification of eucalypt pulp by laccase-mediator. *Enzyme and Microbial Technology*, *39*(6), 1319–1327.

Ibrahim, N. A., Gouda, M., El-shafei, A. M., & Abdel-Fatah, O. M. (2007). Antimicrobial activity of cotton fabrics containing immobilized enzymes. *Journal of Applied Polymer Science*, *104*(3), 1754–1761.

Indrarti, L., & Yudianti, R. (2012). Morphological and thermal properties of alkali treated bacterial cellulose from coconut water. *Indonesian Journal of Materials Science*, *13*(3), 221–225.

Jayakumar, R., Prabaharan, M., Sudheesh Kumar, P. T., Nair, S. V., & Tamura, H. (2011). Biomaterials based on chitin and chitosan in wound dressing applications. *Biotechnology Advances*, *29*(3), 322–337.

Jimenez-Juarez, N., Roman-Miranda, R., Baeza, A., Sánchez-Amat, A., Vazquez-Duhalt, R., & Valderrama, B. (2005). Alkali and halide-resistant catalysis by the multipotent oxidase from Marinomonas mediterranea. *Journal of Biotechnology*, *117*(1), 73–82.

Keshk, S. M. A. S. (2008). Homogenous reactions of cellulose from different natural sources. *Carbohydrate Polymers*, *74*(4), 942–945.

Khan, R. A., Salmieri, S., Dussault, D., Uribe-Calderon, J., Kamal, M. R., Safrany, A., et al. (2010). Production and properties of nanocellulose-reinforced methylcellulose-based biodegradable films. *Journal of Agricultural and Food Chemistry*, *58*(13), 7878–7885.

Kulys, J., Bratkovskaja, I., & Vidziunaite, R. (2005). Laccase-catalysed iodide oxidation in presence of methyl syringate. *Biotechnology and Bioengineering*, *92*(1), 124–128.

Lee, S. J., Kim, S. S., & Lee, Y. M. (2000). Interpenetrating polymer network hydrogels based on poly(ethylene glycol) macromer and chitosan. *Carbohydrate Polymers*, *41*(2), 197–205.

Li, S. M., Fu, L. H., Ma, M. G., Zhu, J. F., Sun, R. C., & Xu, F. (2012). Simultaneous microwave-assisted synthesis, characterization, thermal stability: and antimicrobial activity of cellulose/AgCl nanocomposites. *Biomass & Bioenergy*, *47*, 516–521.

Lin, N., & Dufresne, A. (2014). Nanocellulose in biomedicine: current status and future prospect. *European Polymer Journal*, *59*, 302–325.

Lin, W.-C., Lien, C.-C., Yeh, H.-J., Yu, C.-M., & Hsu, S.-h. (2013). Bacterial cellulose and bacterial cellulose–chitosan membranes for wound dressing applications. *Carbohydrate Polymers*, *94*(1), 603–611.

Lo, J., Lange, D., & Chew, B. (2014). Ureteral stents and foley catheters-associated urinary tract infections: the role of coatings and materials in infection prevention. *Antibiotics*, *3*(1), 87–97.

López-Cruz, J. I., Viniegra-González, G., & Hernández-Arana, A. (2006). Thermostability of native and pegylated *Myceliophthora thermophila* laccase in aqueous and mixed solvents. *Bioconjugate Chemistry*, *17*(4), 1093–1098.

Lynd, L. R., Weimer, P. J., van Zyl, W. H., & Pretorius, I. S. (2002). Microbial cellulose utilization: fundamentals and biotechnology. *Microbiology and Molecular Biology Reviews*, *66*(3), 506–577.

Mohd Amin, M. C. I., Ahmad, N., Halib, N., & Ahmad, I. (2012). Synthesis and characterization of thermo- and pH-responsive bacterial cellulose/acrylic acid hydrogels for drug delivery. *Carbohydrate Polymers*, *88*(2), 465–473.

Mohite, B. V., & Patil, S. V. (2014). A novel biomaterial: bacterial cellulose and its new era applications. *Biotechnology and Applied Biochemistry*, *61*(2), 101–110.

Moosavi-Nejad, S. Z., Rezaei-Tavirani, M., Padiglia, A., Floris, G., & Moosavi-Movahedi, A. A. (2001). Amine oxidase from lentil seedlings: energetic domains and effect of temperature on activity. *Journal of Protein Chemistry*, *20*(5), 405–411.

Mukhopadhyay, A., Dasgupta, A. K., & Chakrabarti, K. (2013). Thermostability: pH stability and dye degrading activity of a bacterial laccase are enhanced in the presence of $Cu_2O$ nanoparticles. *Bioresource Technology*, *127*, 25–36.

Nakai, T., Sugano, Y., Shoda, M., Sakakibara, H., Oiwa, K., Tuzi, S., et al. (2012). Formation of highly twisted ribbons in a carboxymethylcellulase gene-disrupted strain of a cellulose-producing bacterium. *Journal of Bacteriology*, *195*(5), 958–964.

Nieto, M., Nardecchia, S., Peinado, C., Catalina, F., Abrusci, C., Gutiérrez, M. C., et al. (2010). Enzyme-induced graft polymerization for preparation of hydrogels: synergetic effect of laccase-immobilized-cryogels for pollutants adsorption. *Soft Matter*, *6*(15), 3533.

Othman, A., Elshafei, A., Hassan, M., Haroun, B., Elsayed, M., & Farrag, A. (2014). Purification, biochemical characterization and applications of *Pleurotus*

*ostreatus* ARC280 laccase. *British Microbiology Research Journal*, *4*(12), 1418–1439.
Petersen, N., & Gatenholm, P. (2011). Bacterial cellulose-based materials and medical devices: current state and perspectives. *Applied Microbiology and Biotechnology*, *91*(5), 1277–1286.
Poletto, M., Júnior, H., & Zattera, A. (2014). Native cellulose: structure, characterization and thermal properties. *Materials*, *7*(9), 6105–6119.
Poonkuzhali, K., Sathishkumar, P., Boopathy, R., & Palvannan, T. (2011). Aqueous state laccase thermostabilization using carbohydrate polymers: effect on toxicity assessment of azo dye. *Carbohydrate Polymers*, *85*(2), 341–348.
Quan, D., Kim, Y., & Shin, W. (2004). Characterization of an amperometric laccase electrode covalently immobilized on platinum surface. *Journal of Electroanalytical Chemistry*, *561*(1–2), 181–189.
Römling, U., & Galperin, M. Y. (2015). Bacterial cellulose biosynthesis: diversity of operons, subunits, products, and functions. *Trends in Microbiology*, *23*(9), 545–557.
Santos, C., Silva, C. J., Buttel, Z., Guimaraes, R., Pereira, S. B., Tamagnini, P., et al. (2014). Preparation and characterization of polysaccharides/PVA blend nanofibrous membranes by electrospinning method. *Carbohydrate Polymers*, *99*, 584–592.
Saska, S., Teixeira, L. N., de Oliveira, P. T., Gaspar, A. M. M., Ribeiro, S. J. L., Messaddeq, Y., et al. (2012). Bacterial cellulose-collagen nanocomposite for bone tissue engineering. *Journal of Materials Chemistry*, *22*(41), 22102–22112.
Sathishkumar, P., Kamala-Kannan, S., Cho, M., Kim, J. S., Hadibarata, T., Salim, M. R., & Oh, B.-T. (2014). Laccase immobilization on cellulose nanofiber: the catalytic efficiency and recyclic application for simulated dye effluent treatment. *Journal of Molecular Catalysis B: Enzymatic*, *100*, 111–120.
Shah, N., Ul-Islam, M., Khattak, W. A., & Park, J. K. (2013). Overview of bacterial cellulose composites: a multipurpose advanced material. *Carbohydrate Polymers*, *98*(2), 1585–1598.
Strong, P. J., & Claus, H. (2011). Laccase: a review of its past and its future in bioremediation. *Critical Reviews in Environmental Science and Technology*, *41*(4), 373–434.
Sulaiman, S., Mokhtar, M. N., Naim, M. N., Baharuddin, A. S., & Sulaiman, A. (2014). A review: potential usage of cellulose nanofibers (CNF) for enzyme immobilization via covalent interactions. *Applied Biochemistry and Biotechnology*, *175*(4), 1817–1842.
Taraszkiewicz, A., Fila, G., Grinholc, M., & Nakonieczna, J. (2013). Innovative strategies to overcome biofilm resistance. *BioMed Research International*, 1–13.
Tavares, A. P. M., Silva, C. G., Dražić, G., Silva, A. M. T., Loureiro, J. M., & Faria, J. L. (2015). Laccase immobilization over multi-walled carbon nanotubes: kinetic: thermodynamic and stability studies. *Journal of Colloid and Interface Science*, *454*, 52–60.
Thallinger, B., Prasetyo, E. N., Nyanhongo, G. S., & Guebitz, G. M. (2013). Antimicrobial enzymes: an emerging strategy to fight microbes and microbial biofilms. *Biotechnology Journal*, *8*(1), 97–109.
Turner, B. L. (2010). Variation in pH optima of hydrolytic enzyme activities in tropical rain forest soils. *Applied and Environmental Microbiology*, *76*(19), 6485–6493.
Villa, T. G., & Crespo, P. V. (2010). *Enzybiotics: antibiotic enzymes as drugs and therapeutics*. Hoboken, NJ, USA: Wiley.
Vu, N. K., Zille, A., Oliveira, F. R., Carneiro, N., & Souto, A. P. (2013). Effect of particle size on silver nanoparticle deposition onto dielectric barrier discharge (DBD) plasma functionalized polyamide fabric. *Plasma Processes and Polymers*, *10*(3), 285–296.
Wu, S.-C., & Lia, Y.-K. (2008). Application of bacterial cellulose pellets in enzyme immobilization. *Journal of Molecular Catalysis B: Enzymatic*, *54*(3–4), 103–108.
Yao, W., Wu, X., Zhu, J., Sun, B., & Miller, C. (2013). In vitro enzymatic conversion of γ-aminobutyric acid immobilization of glutamate decarboxylase with bacterial cellulose membrane (BCM) and non-linear model establishment. *Enzyme and Microbial Technology*, *52*(4–5), 258–264.
Zille, A., Fernandes, M. M., Francesko, A., Tzanov, T., Fernandes, M., Oliveira, F. R., et al. (2015). Size and aging effects on antimicrobial efficiency of silver nanoparticles coated on polyamide fabrics activated by atmospheric DBD plasma. *ACS Applied Materials & Interfaces*, *7*(25), 13731–13744.